ELSEVIER

Journal of Power Sources 54 (1995) 511–515

JOURNAL OF POWER SOURCES

Crystal structure study of $LiNi_{1-x}Mn_xO_2$

Yoshiaki Nitta, Kazuhiro Okamura, Kazunori Haraguchi, Shigeo Kobayashi, Akira Ohta

Technology Laboratory, Matsushita Battery Industrial Co., Ltd., 1 Matsushita-cho, Moriguchi, Osaka 570, Japan

Abstract

Manganese in an $LiNi_{1-x}Mn_xO_2$ mixed valence compound, provided a layered structure of $LiNiO_2$ ($R\bar{3}m$) substituting a part of the 3*a* site to manganese was found to exist in part of the nickel site by using XAFS measurement and Rietveld analysis, and the majority of manganese existed in a divalent state by using electron spin resonance measurement. This material has less overvoltage than $LiNiO_2$ at the end of charging state. It is presumed that control of the mixed valence affects the electron occupation state of the valence band, mainly e_g orbit, and the crystal field, providing an action/relaxing change of the electron occupation state of the valence band according to the charge/discharge reaction.

Keywords: Lithium; Manganese; Nickel; Crystal structure

1. Introduction

These days, $LiNiO_2$ of a layered structure (space group $R\bar{3}m$) as a new cathode material for lithium secondary battery has been studied intensively. However, when a cathode material of a layered structure is in its charging state, its crystal or electronic structure shows a peculiar behaviour [1] and, especially, in the case of $LiNiO_2$ its electronic conductivity has been lowered in view of its electron state. Under such circumstances, Robin and Day [2] tried a mixed valence control ($LiNi_{1-x}M_xO_2$) substituting a part of the Ni layer (3*a* site) for other elements, in order to stabilize Ni in a higher-order oxidation state and keeping the basic structure of $LiNiO_2$. After having examined several elements that enable this substitution, we found Mn (20 wt.% to Ni) of 3d transition metal element as the most effective element.

For $LiNi_{1-x}Mn_xO_2$ ($x=0.2$) with $R\bar{3}m$ structure thus obtained, we found by Rietveld analysis that Mn is substituted for a part at the 3*a* site to be solid solution, and consequently, the electronic structure and charge/discharge properties are greatly affected. Specifically, charge-transfer resistance in the charging state (4.3 V versus Li) could be restricted to ~50% of $LiNiO_2$. Further, it was found that the crystal structure changes as the charge/discharge reaction proceeds while mostly keeping the $R\bar{3}m$ structure without making a monoclinic crystallization.

This report gives a synthesis method of $LiNi_{1-x}Mn_xO_2$ ($x=0.2$), and various properties of the obtained specimen, comparing with those of $LiNiO_2$. Also, the state of Mn in $LiNi_{1-x}Mn_xO_2$ ($x=0.2$) has been determined, and the effect on the electrochemical properties has been examined.

2. Experimental

$Ni(OH)_2$ as the Ni compound and LiOH and Li_2CO_3 as the Li compound, and $MnCO_3$ in the case of adding Mn were weighted; then, they were synthesized at 700–850 °C in an O_2 atmosphere. Crystal phase change in the reaction process from the starting materials to the final products were observed by high-temperature X-ray diffraction methods. Mn solid solution of the obtained $LiNi_{1-x}Mn_xO_2$ ($x=0.2$) was examined by powder XRD method and Rietveld analysis. Valencies of Mn and Ni in the specimen, their binding energy and coordination states were studied by electron spin resonance (ESR), X-ray photoelectron spectroscopy (XPS) and X-ray absorption fine structure (XAFS) analysis methods, comparing with those of $LiNiO_2$.

Charge/discharge properties of the specimen were obtained by measuring with a three-electrode method at constant current, at a current density 0.5 mA/cm^2,

SSDI 0378-7753(94)02137-R

charge/discharge range of 3.0 to 4.3 V (Li standard) at room temperature. As electrolyte, 1 M $LiPF_6$ in ethylene carbonate–diethyl carbonate (EC–DEC) 1 M $LiClO_4$ in propylene carbonate (PC) was used.

3. Results and discussion

3.1. Synthesis

Fig. 1 shows the results of high-temperature XRD in the synthesis process of $LiNi_{0.8}Mn_{0.2}O_2$. Starting materials were $MnCO_3$, $Ni(OH)_2$ and LiOH. Up to around 300 °C, peaks attributing to these materials are observed. Between 300 and 700 °C, a two-phase coexistent crystal phase zone of the peak, attributed to the rock-salt-type Ni oxide and Mn oxide including Li, exists. From at 700 to 750 °C, a phase change to a single substance of $R\bar{3}m$ structure begins. At around 850 °C, the $R\bar{3}m$ layer structure is mostly completed, and in higher temperature areas, $R\bar{3}m$ is kept without great change.

Fig. 2 shows the relation between the discharge capacity and the peak ratio of (006)/(101) in $LiNi_{0.8}Mn_{0.2}O_2$. The discharge capacity is rapidly increased when the peak ratio is below 1.0. Preferably, to obtain a high capacity, the value of the peak ratio is between 0.34 and 0.4.

Fig. 3 shows the results of the effect of the presence/absence of Mn addition to $LiNiO_2$ on the synthesis conditions. This Figure shows the relation of the final synthesis temperature and the peak ratio of (006)/(101) which is one of the lattice parameters showing a completion degree of the $R\bar{3}m$ crystal structure, including an evaluation factor of the electrochemical activity.

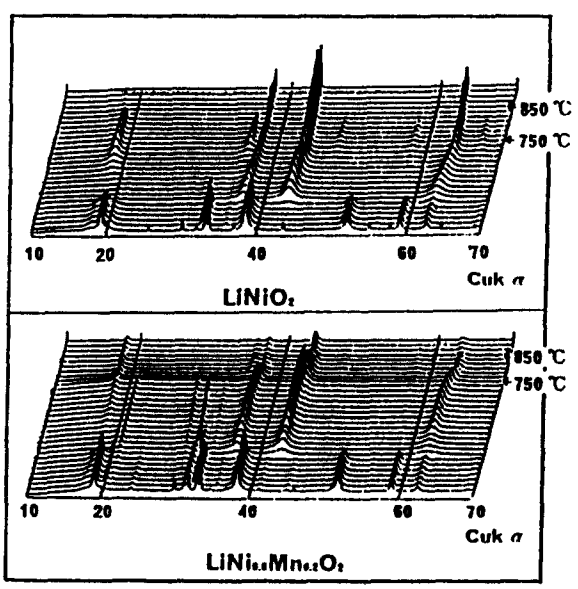

Fig. 1. High-temperature X-ray diffraction analysis for the preparation of $LiNiO_2$, $LiNi_{0.8}Mn_{0.2}O_2$.

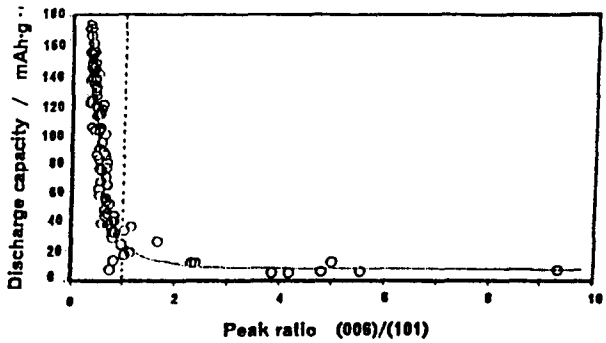

Fig. 2. Discharge capacity vs. peak ratio of (006)/(101).

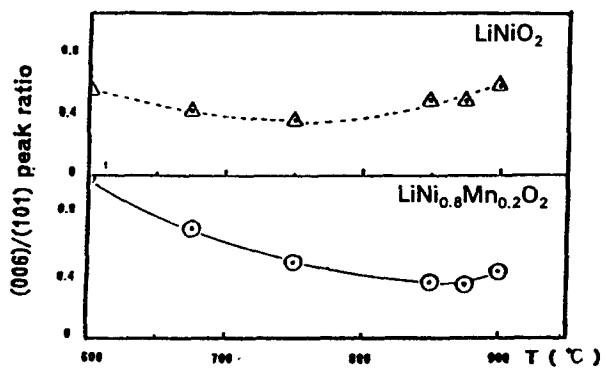

Fig. 3. Discharge temperature vs. peak ratio of (006)/(101).

Table 1
Results of the Rietveld analysis

Sample	Lattice constants		R_{wp}	$R.I.$
	a	c		
$LiNiO_2$	2.8769	14.1983	15.70	2.78
$LiNi_{0.8}Mn_{0.2}O_2$	2.8776	14.2305	16.45	2.97

$LiNi_{0.8}Mn_{0.2}O_2$ has a minimum peak strength ratio at around 850 °C, and has a maximum electrochemical activity, whereas, $LiNiO_2$ has a minimum peak strength ratio at around 750 °C. Thus, both of them have different synthesis processes. For synthesizing $LiNi_{0.8}Mn_{0.2}O_2$, temperature conditions must be about 100 °C higher than those of $LiNiO_2$.

A solid solution of Mn in $LiNi_{0.8}Mn_{0.2}O_2$, thus obtained, was analysed by crystalline structure analysis, by powder XRD method and Rietveld analysis. The results showed that $LiNi_{0.8}Mn_{0.2}O_2$ belongs to $R\bar{3}m$ and a part of Ni ($3a$ site) is substituted for Mn. Table 1 shows the results of the Rietveld analysis.

3.2. Characterization of $LiNO_2$ and $LiNi_{0.8}Mn_{0.2}O_2$

The electron spin state of the valence band was examined. Fig. 4 shows the results of the Curie–Weiss plots by using magnetic balance. It shows that the relation of $1/\chi$ and temperature in both compounds

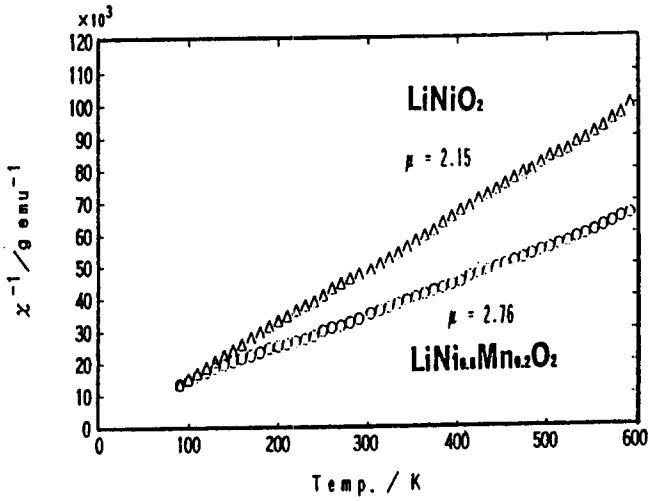

Fig. 4. Curie–Weiss plots of $LiNiO_2$ and $LiNi_{0.8}Mn_{0.2}O_2$.

includes room temperature area, obtaining linear relation, and both are paramagnetic substances achieving the Curie–Weiss law. The magnetic moment μ calculated by the linear slope is 2.15 in $LiNiO_2$, and 2.76 in $LiNi_{0.8}Mn_{0.2}O_2$. When Ni at the 3*a* site is 3*d*7 low-spin state, then μ is 1.73; therefore, both compounds have large numeric values and among others, Mn solid solution becomes larger. This shows that the localized d electron in the valence band has a large effective electron-spin amount accordingly. It was also seen that charging these specimens up to 4.3 V versus Li caused an increase in the individual μ values.

Fig. 5 shows XPS spectrum of the valence band. The results were divided into 5 peaks, and fitting was performed. The peak near 0 eV mainly shows bond energy relating to σ-bond with oxygen, and the inner peaks show bond energy relating to π-bond with oxygen [3]. Comparing both compounds, the overall peak position is shifted to higher energy site in $LiNi_{0.8}Mn_{0.2}O_2$. The results are shown in Table 2.

These results suggested that in Mn solid solution, the bond energy of the valence band is shifted to 0.3–0.5 eV high energy site, the effects on the Fermi level by a mixed valence are estimated. Then, for studying the existence state of Mn in $LiNi_{0.8}Mn_{0.2}O_2$, the Mn valence and the coordination state were examined with electron spin resonance (ESR) and XAFS.

Fig. 6 shows the ESR spectrum. Analysing this spectrum, a signal with about 20*mT* line width is observed in 337*mT*. Assuming that this signal is Mn^{4+}, $s=3/2$ is obtained, and ESR spectrum reflecting a quadrupole state must be observed, but the signal seen around 337*mT* is not considered to be a quadrupole state spectrum, in view of the *g* value and the linear state. Therefore, it is presumable that this signal is caused by Mn^{2+}. Moreover, assuming that the spin state of $LiNiO_2$ to be Ni^{3+} ($s=1/2$), the amount of spin from the ESR spectrum was determined by using a standard

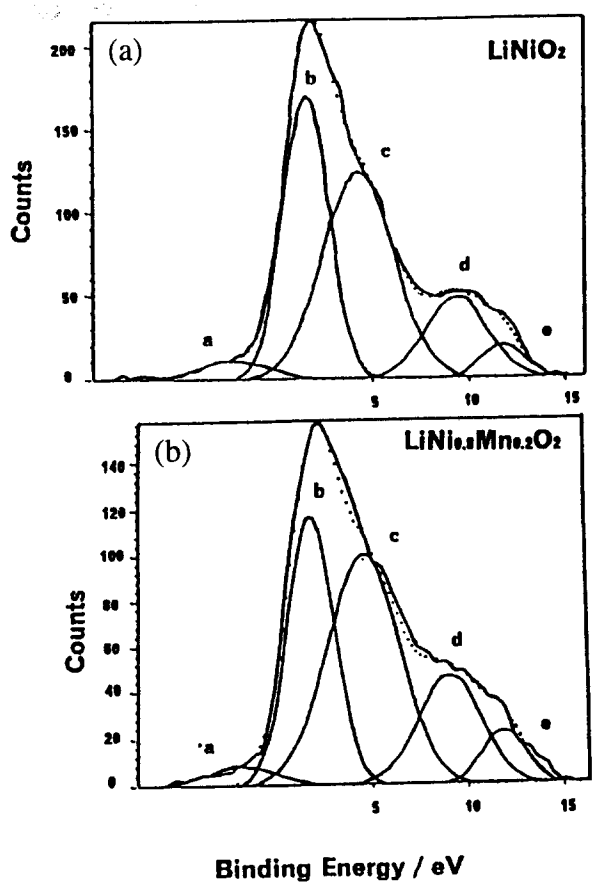

Fig. 5. X-ray photoelectron spectroscopy spectrum of the valence bands: (a) $LiNiO_2$, and (b) $LiNi_{0.8}Mn_{0.2}O_2$.

Table 2
Results of XPS spectrum (eV)

Sample	Peak a	Peak b	Peak c	Peak d	Peak e
$LiNi_{0.2}$	−2.15	1.63	4.23	9.44	11.84
$LiNi_{0.8}Mn_{0.2}O_2$	−1.65	1.95	4.54	9.13	11.94
Difference	0.5	0.32	0.31	0.31	0.10

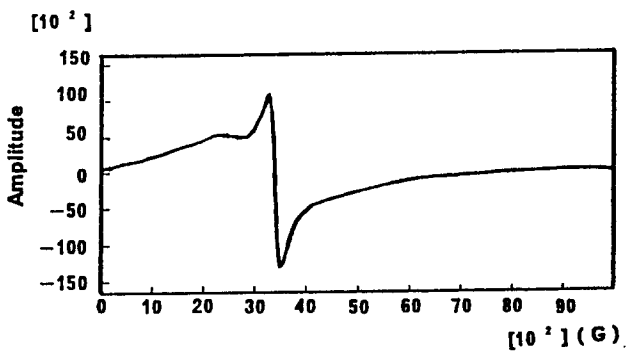

Fig. 6. Electron spin resonance of $LiNi_{0.8}Mn_{0.2}O_2$.

specimen $CuSO4 \cdot 5H_2O$ single crystal, and Ni^{3+}($s=1/2$) in $LiNiO_2$ was found to be presented by 65% of the whole Ni amount, and it was known to decrease to 14% when charging up to 4.3 V versus Li. Therefore,

the valence state of $LiNiO_2$ is not a simple Ni^{3+} ($s = 1/2$), which is supposed to depend greatly on the Li amount in the lattice.

Fig. 7 shows the results of the spectrum analysis of XAFS imaginary part at the Ni/K absorption edge and Mn/K absorption edge. These results show that structure around Ni in $LiNi_{0.8}Mn_{0.2}O_2$ solid phase does not have a particular difference from that of $LiNiO_2$, and that the structure around Mn is quite similar; that is, it is presumed that most of the Mn is substituted for Ni at the 3*a* site and has almost the same coordinating number.

Fig. 8 shows the results of the closest distance between metal and oxygen. A calculation program FEFF 3.25 [5] used an single-scattering, curved wave XAFS spectrum. It was found that these two distances, 1.85 and 2.04 Å, present Ni–O in $LiNiO_2$. This result nearly coincides with the result reported by Pickering et al. [4]. It was discovered that addition of Mn causes a change in the Ni–O distances, 1.67 and 2.08 Å, respectively.

Hence, the factor that shows two different distances between metal and oxygen could be the presence of two valence states of the metal ion, or the difference in the radius ratio of two ions due to the existence of a hole on oxygen. That is, Ni ion could be present in the forms of Ni^{3+} and Ni^{2+}, and when Mn has a larger ion radius than Ni, different states of the valence band from Ni ion, is present at the 3*a* site as solid solution, it can change substantially the distance between Ni and oxygen.

Meanwhile, the Mn–O distance also indicated two distances of 1.89 and 2.39 Å, providing a partial substitution at the 3*a* site in the same crystal structure. So the valence of Mn is not completely present as

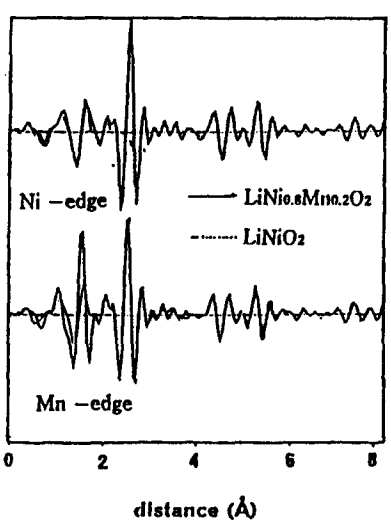

Fig. 7. EXAFS spectrum of $LiNi_{0.8}Mn_{0.2}O_2$.

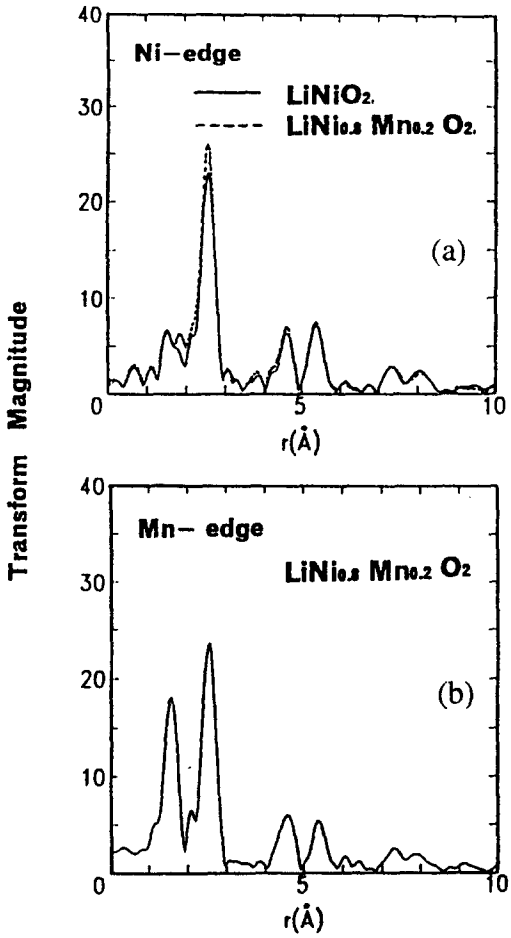

Fig. 8. The Fourier-transform of the (a) Ni and (b) Mn/K edge EXAFS spectra of $LiNiO_2$ and $LiNi_{0.8}Mn_{0.2}O_2$.

Mn^{2+} (low spin), but it shows partly a different valence state. It was found, as other recognition, that while the Ni–Ni distance shows the same 2.89 Å in $LiNiO_2$ and $LiNi_{0.8}Mn_{0.2}O_2$, the Ni–Mn distance is 2.91 Å in $LiNi_{0.8}Mn_{0.2}O_2$.

3.3. Discharge property

Fig. 9 shows the discharge properties of the specimen. In $LiNiO_2$, after a potential drop of ~100 mV in the initial discharge time, the potential plateaued at around 4.10–4.05 V in the course of the discharge reaction, whereas, in $LiNi_{0.8}Mn_{0.2}O_2$, after a potential drop of ~50 mV, the potential decreases gradually without a plateau area. This indicates that $LiNi_{0.8}Mn_{0.2}O_2$ shows a different electron state from that of $LiNiO_2$ in the charging state, and specifically, the electronic conductivity in the initial discharge time has made considerable progress. Since the discharge curve is more uniform,

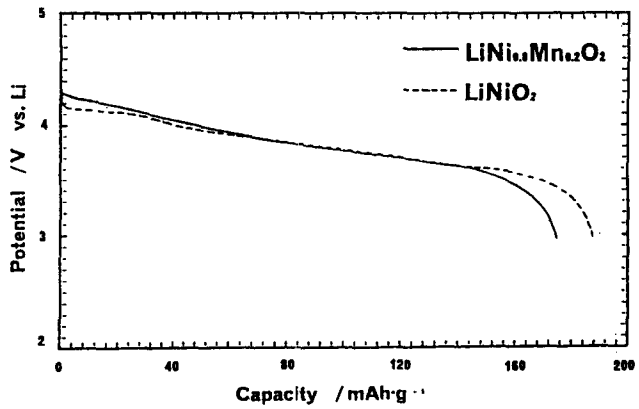

Fig. 9. Discharge characteristics of $LiNi_{0.8}Mn_{0.2}O_2$ and $LiNiO_2$. Charge/discharge conditions: current density = 0.5 mA cm^{-1}; potential = 3.0–4.3 V, and electrolyte = 1 M $LiPF_6$/EC–DEC.

it is presumed that the active material performing discharge reaction is displaced to a substance of a more homogeneous phase-reaction property.

4. Conclusions

The electrochemical properties of a compound can be characterized by the acquisition of a mixed valence compound adding Mn. That is, it is presumed that the control of a mixed valence affects the electron occupation state of the valence band, mainly the e_g orbit, and the crystal field, providing an action/relaxing change of the electron occupation state of the valence band according to the charge/discharge reaction.

References

[1] J.N. Reimer and J.R. Dahn, *J. Electrochem. Soc., 139* (1992) 2091.
[2] M.B. Robin and P. Day, *Adv. Inorg. Chem., 10* (1967) 247.
[3] J. Van Elp, H. Eskes, P. Kniper and G.A. Sawatzky, *Phys. Rev. Sect. B, 45* (1992) 1612.
[4] I.J. Pickering, G.N. George, J.T. Lewandowski and A.J. Jacobson, *J. Am. Chem. Soc., 115* (1993) 4137.
[5] J.J. Rehr, R.C. Albers and J. Mustre de Leon, *Phys. Rev. Sect. B, 158* (1989) 417.